Polymer Bulletin (2024) 81:1421–1437
https://doi.org/10.1007/s00289-023-04768-8

ORIGINAL PAPER

Synthesis and cytotoxic activities of selenium nanoparticles incorporated nano-chitosan

Ahmed E. Abdelhamid[1] · Eman H. Ahmed[1] · Hanem M. Awad[2] · Magdy M. H. Ayoub[1]

Received: 24 September 2022 / Revised: 9 March 2023 / Accepted: 17 March 2023 /
Published online: 6 April 2023

Abstract

New system compromising of chitosan nanoparticles encapsulated pre-synthesized selenium nanoparticles in the presence of 5-fluorouracil was successfully prepared and used for cancer antiproliferation. Selenium nanoparticles were synthesized using ascorbic acid as reducing agent under mild condition. Chitosan nanoparticles were prepared via ionic gelation technique using sodium tri-polyphosphate. Characterization of the prepared nanoparticles was carried out using FTIR, TEM, XRD, TGA and dynamic light scattering (DLS). The results displayed the formation of selenium nanoparticles with an average size 20 nm and chitosan nanoparticles with an average size 207 and 250 nm for neat nano-chitosan and chitosan incorporated 5-fluorouracil/selenium nanoparticles, respectively. The encapsulated nanocomposites were tested for treatment of cancer cell of human colorectal carcinoma (HCT-116), human liver carcinoma (HepG-2), and human breast adenocarcinoma MCF-7. The results indicated the potent cytotoxic activities of all nanocomposite toward the tested cells with enhanced anticancer activity rather than the single drug or neat selenium nanoparticle. All composites were tested against non-tumor fibroblast-derived cell line (BJ) and demonstrated very low cytotoxicity.

Keywords Chitosan nanoparticles · Selenium nanoparticles · 5-Fluorouracil · Anticancer · Drug delivery

✉ Ahmed E. Abdelhamid
ahmednrc10@gmail.com

[1] Polymers and Pigments Department, National Research Centre, 33 El-Buhouth St., Dokki, Giza 12622, Egypt

[2] Tanning Materials and Leather Technology Department, National Research Centre, Dokki, Giza 12622, Egypt

Introduction

Chitosan is renewable natural polysaccharide obtained from deacetylation of chitin, and it contains many reactive functional groups as –OH and $–NH_2$ [1, 2]. Chitosan is well characterized as a biodegradable, biocompatible, hydrophilic, non-immunogenic, nontoxic and cost effective polymer. Thus, it is currently being intensively used in food, agriculture, biotechnology and pharmacy [3]. Chitosan can be easily converted onto nanoparticles using different techniques such as ionic gelation, emulsion droplet coalescence, emulsion solvent diffusion, reverse micellar method, polyelectrolyte complexation and desolvation [4–6]. All these methods comprise bottom-up fabrication processes, which involve the assembly of molecules in solution to form defined structures (nanoparticles). Chitosan nanoparticles (ChNPs) are being used extensively for drug delivery applications because of its favorable properties such as the ability to bind with organic compounds, susceptibility to enzymatic hydrolysis, and intrinsic physiological activity [7]. The drug encapsulation and release characteristics of ChNPs are largely dependent on their size, surface potential, molecular weight and stability [8, 9].

Another promising material is selenium. Selenium is a necessary micronutrient for man health and it is derived from many sources as meats, fish and plants [10]. Selenium deficiency has been linked to variety of human diseases like cardiomyopathy [11]. Selenium nanoparticles (SeNPs) (the red zero valent selenium) showed an excellent antioxidant activity, disease prevention effects and a great deal of attention as a potential cardio protective and therapeutic agent [12].

In the recent years, selenium nanoparticles (SeNPs) have gained increasing attention, due to their noticeable biological activities and biosafety performance [13]. There are different methods for preparing SeNPs using physical, chemical or biological techniques. The main method is by using the chemical-reduction method, involving many reducing materials such as ascorbic acid, hydrazine, sodium citrate, and sodium borohydride [14–18]. SeNPs represent significant prospective for technological applications in different fields such as medicine, diagnosis, therapy, electronic devices, catalysis and chemical sensors, because of their unique optical, electronic, electrocatalytic and biological properties [19]. SeNPs without stabilization can be easily aggregated and affect their applications. Many studies have been discovered that the surface modification of SeNPs is significantly influenced with polysaccharide compounds [20].

Zeng et al. [21] found that SeNPs stabilized by polysaccharides that extracted from mushrooms can be applied to control the anticancer activities. Besides controlled release of selenium, cell absorption and targeting activity, the accessibility and preparation convenience are also important characteristics of the carrier materials in practical applications [22, 23]. Some previous studies suggested that selenium nanoparticles stabilized by pure chitosan could inhibit cancer cells; however, this hypothesis has not been confirmed in vivo. Moreover, the effect of chitosan molecular weight on SeNPs release and valence state transformation of Ch-SeNPs in vitro has also been neglected in previous studies [24].

The goal of the present work was focused on investigation of selenium nanoparticle stabilization within chitosan nanoparticles combined with well-known anticancer drug; 5-Fluorouracil for using as anti-proliferative for Cancer Cells. To achieve this goal, chemical reduction of selenous acid using ascorbic acid was performed. The ionic gelation technique was used to prepare chitosan nanoparticles in the presence and absence of SeNPs and 5-Fluorouracil. Characterization of the new composite of ChNPs incorporated SeNPs and 5 fluorouracil was explored and their evaluation for cancer treatment activity was investigated.

Materials and methods

Materials

Chitosan (low molecular weight; < 100 KDa, Bioscience company). Sodium tripolyphosphate, 5-Fluorouracil, Selenous acid and Ascorbic acid were delivered from Aldrich. Acetic acid was analytical grade supplied from Adweck.

Preparation of selenium nanoparticles

Selenium nanoparticles (SeNPs) were prepared by chemical reduction of Selenous acid using ascorbic acid. A weight of 0.25 g Selenous acid was dissolved in 50 ml distilled water under stirring and the temperature of this solution was raised to 60 °C. Ascorbic acid (0.025 g) was dissolved in 20 ml distilled water and added to the warm solution of selenous acid under stirring for about 10 min. The solution color was turned into red color indicating the formation of selenium nanoparticles.

Preparation of chitosan- selenium nanocomposites

Chitosan nanoparticles were prepared by ionic gelation method using sodium tripolyphosphate (TPP) as described in literature [25, 26]. Briefly; dilute solution of the low molecular weight chitosan (0.5 g) was dissolved in 2% aqueous acetic acid (100 ml) under stirring at room temperature till complete dissolution. 0.25 g of TPP was dissolved in distilled water under stirring. The TPP solution was added dropwise to chitosan solution under continuous stirring and after complete addition the solution mixture left under stirring for about additional one hour. Turbid solution of chitosan nanoparticles was obtained. For encapsulation of selenium nanoparticles, the same procedure was used instead 10 or 20% (respect to chitosan weight) of selenous acid was added to the dissolved chitosan solution under heat at 60 °C then ascorbic acid was added dropwise and finally gelation with TPP was performed. For

encapsulation 5-Fluorouracil drug, 10 mg or 20 mg that dissolved in 10 ml water for each was added to chitosan solution and apply the same procedure.

In vitro fluorouracil release

The drug release studies from the synthesized nanocomposite were performed in 0.1 M phosphate buffer solution (PBS) with two different pH (pH: 4 and 7.4) simulating the acidic and blood pH, respectively. 50 mg from the nanocomposite (Ch-Se10-Flu20) with relatively high initial drug concentration was suspended in 2 ml buffer solution and transfer onto dialysis bag with molecular weight cut off (12–14 KDa), then the dialysis bag was soaked in 50 ml PBS reservoir with mild agitation (100 rpm). One ml of the phosphate buffer reservoir was taken out at different time interval and fresh buffer was added to stimulate drug release from the nanocomposite. The amount of the released drug was determined using UV spectrophotometer at wavelength 266 nm [27].

Characterization of nano-particles

Chitosan nanoparticles with their encapsulated particles were characterized using FTIR, TEM, DLS, DSC and X-ray as following:

Fourier transform infrared spectroscopy (FT-IR)

The reactive functional groups of the prepared nanoparticles were explored using Fourier transform infrared spectroscopy FTIR (Jasco, FT/IR 6100, Japan) within the spectral range of 4000–400 cm^{-1}.

Transmission electron microscopy (TEM)

The shape and size of the prepared nanoparticles was examined using TEM measurements [Jeol- TEM- 2100 high resolution- transmission electron Microscopy, Japan]. Transmission electron microscopy was running at magnification power: 200 kv, maximum resolution: 1.4 A°.

Zeta-potential and particles size measurements

Zeta potential and particles size of the prepared nanoparticles were investigated using dynamic light scattering (DLS) technique via Zeta-sizer (Nano ZS, Malvern Instruments Ltd., Malvern, UK). The prepared nanoparticles were appropriately diluted before measurements. Then the samples were transferred to a 4 ml quartz cuvette and measured at room temperature (25 °C). Size distributions were investigated in terms of intensity versus particle size.

Thermal gravimetric analysis (TGA)

Thermal gravimetric analysis (TGA) is the most frequently used to evaluate thermal stability of the nanoparticles which used in drug delivery. The measurements were carried out using (TGA- DSC- SDT Q600 V20.9 Build 20, USA) instrument in the range from room temperature up to 700 °C. The heating rate was 10 °C/min under inert nitrogen (N_2) atmosphere. The Tg is easily determined by DSC which allows the detection of endothermic and exothermic effects.

X-ray diffraction (XRD)

XRD is a technique usually used to investigate the crystallinity of the prepared nanoparticles and identify the physical state of the materials; hence confirm the formation and presence of certain nanoparticle. XRD measurements were performed with X-ray diffractometer (Bruker D8 Advance, USA).

Cell culture conditions

Three cancer cell lines were used to evaluate the anticancer activity of Ch/Se nanocomposite. Human colorectal carcinoma (HCT-116), human liver carcinoma (HepG-2), and human breast adenocarcinoma (MCF-7) in addition to the normal human skin fibroblast (BJ-1) cell line were purchased from the American Type Culture Collection (Rockville, MD, USA) and maintained in Dulbecco's Modified Eagle's Medium (DMEM) supplemented with 10% heat-inactivated fetal bovine serum (FBS), 100 U mL^{-1} penicillin, and 100 U mL^{-1} streptomycin. The cells were grown at 37 °C in a humidified atmosphere of 5% CO_2.

MTT Antiproliferative assay

The antiproliferative activities on the HepG-2, HCT-116, MCF-7 and BJ-1 were estimated by the 3-[4,5-dimethyl-2-thiazolyl)-2,5-diphenyl-2H-tetrazolium bromide (MTT) assay. This test is based on MTT cleavage by mitochondrial dehydrogenases form viable cells [28–30]. Cells were placed in a 96 well sterile microplate (5×10^4 cells $well^{-1}$) and incubated at 37 °C in serum-free media containing dimethyl sulfoxide (DMSO) and either a series of various concentrations of each compound or doxorubicin (positive control) for 48 h before the MTT assay. After incubation, the media were removed and 40 µL MTT (2.5 mg mL^{-1}) was added to each well. Incubation was resumed for an additional 4 h. The purple formazan dye crystals were solubilized with 200 µL DMSO. Absorbance was measured at 590 nm in a Spectra Max Paradigm Multi-Mode microplate reader (Molecular Devices, LLC, San Jose, CA, USA). Relative cell viability was expressed as

the mean percentage of viable cells compared to the untreated control cells. All experiments were conducted in technical triplicate and three biological replicates. All values were reported as mean ± SD. IC_{50} were determined by SPSS Inc probit analysis (IBM Corp., Armonk, NY, USA).

Results and discussions

Characterization of the prepared nanocomposite

The prepared chitosan encapsulated selenium nanoparticles in the presence or absence of 5-fluoruracil were investigated and characterized by different instrumental techniques. Figure 1 indicates the FTIR of the prepared chitosan nanoparticles, and it is clearly observed that the ChNPs showed broad band at 3420 cm^{-1} corresponding to the stretching of intermolecular bonded OH combined with NH groups. A small sharp band at 3720 cm^{-1} revealed to free OH groups. The asymmetric and symmetric stretching vibrations were appeared at 2911 and 2858 cm^{-1} corresponding to the aliphatic CH_2 groups, respectively. However, the peaks at 1631 cm^{-1} and 1380 cm^{-1} were attributed to N–H bending and OH bending, respectively. The peak at 1045 cm^{-1} was corresponding to C–O stretching. The FTIR spectra of Ch-SeNPs showed blue shift for the characteristic peak of O–H group at 3420 cm^{-1} to (3425.26 cm^{-1}). Moreover, a slight shift in the absorption peaks of chitosan 3434.55 (O H stretch), 2924.13 (C H stretch), 1734.28 (COO stretch), 1070.77 cm^{-1} (C O stretch) after Se nanoparticles incorporation. The shift of OH band might indicate

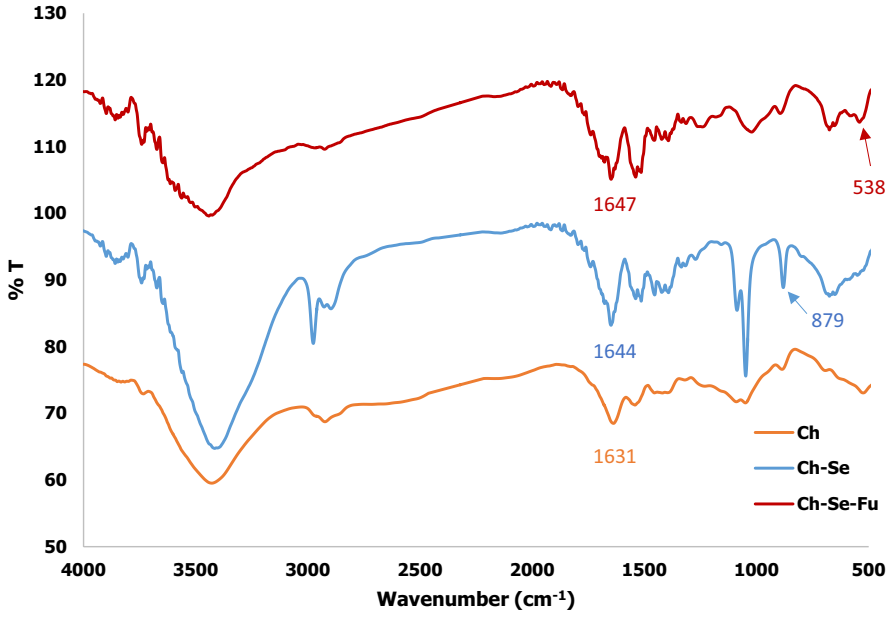

Fig. 1 FTIR of ChNPs, ChNPs-Se and ChNPs-Se-Flu

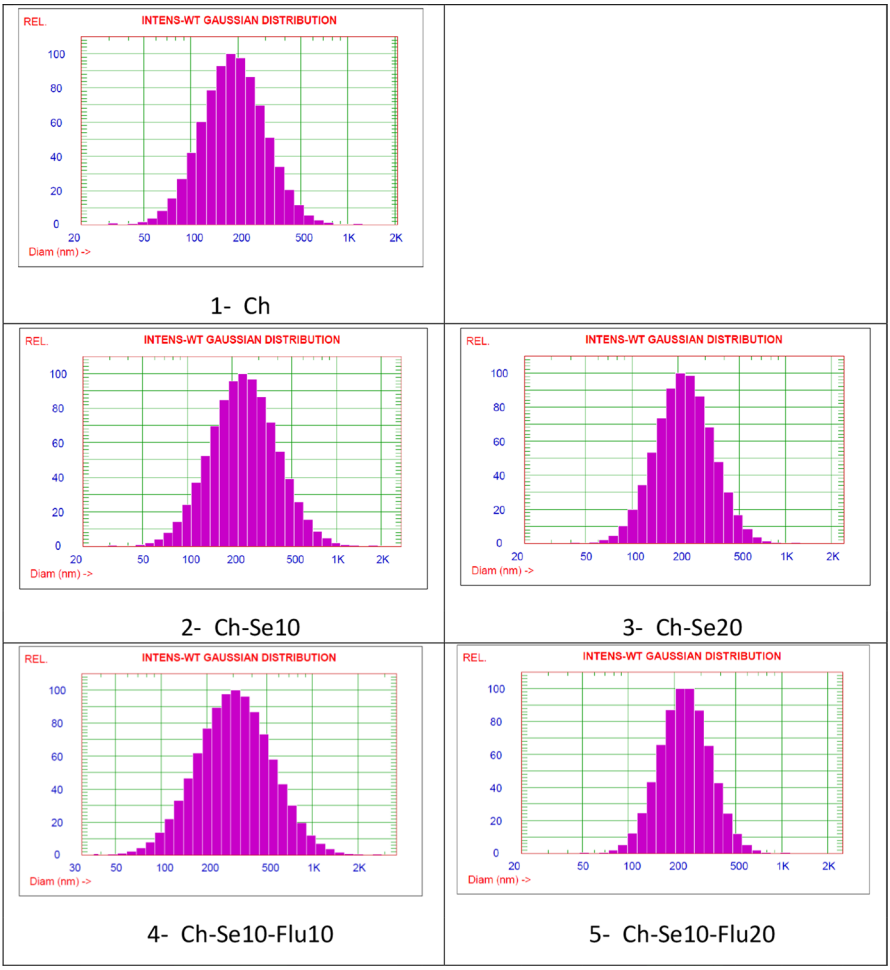

Fig. 2 Average Particles size of **a** Ch-NP, **b** Ch-Se10, **c** Ch-Se20, **d** Ch-Se10-Flu10 and **e** Ch-Se10-Flu20

Table 1 Average of particle size and zeta potential of (a) Ch-NP, (b) Ch-Se10, (c) Ch-Se20, (d) Ch-Se10-Flu10 and (e) Ch-Se10-Flu20

Sample	Size (nm)	Zeta potential (mV)
Ch	207.4	38.96
Ch-Se-10	271.5	23.91
Ch-Se-20	239.5	31.32
Ch-Se-10-Flu-10	251.3	41.02
Ch-Se-10-Flu-20	358.2	31.06

an interaction between hydroxyl groups of chitosan and surface of SeNPs. The peak at 1631 cm^{-1} was clearly appeared and shifted to 1644 cm^{-1}, indicating the formation of Se–O bond. Another band at 879 cm^{-1} was attributed to the Se–O stretching vibrations [22]. The combination mode of chitosan and SeNPs was similar to what was reported previously [8]. A weak peak at 538 cm^{-1} revealed to C–F group of 5-fluorouracil in Ch–Se–Fu sample.

The particle size and zeta potential measurements were determined using DLS analysis as shown in Fig. 2 and Table 1. The results indicated that the average values of particle size for Ch, Ch-Se10, Ch-Se20, Ch-Se10-Flu10 and Ch-Se10-Flu20 were 207.4, 271.5, 239.5, 251.3 and 358.2 nm, respectively. The total size of nanochitosan was slightly increased from 207.4 to 271.7 nm as clearly observed in Fig. 2 after incorporation of selenium nanoparticle. Such increment might be considered good indication for the nanoparticles stability [8]. Nevertheless, the dramatic increase in the particle size of Ch-Se10-Flu20 might be attributed to the higher of 5Flu concentration. However, for the lower concentration of drug it was 251.3 nm indicating that Ch-Se10-Flu10 was highly recommended candidate for obtaining more disperse nano-capsules.

The Zeta potential of dispersion is measured by applying an electric field across the dispersion. The Zeta potential is the potential difference existing between the surface of a solid particle immersed in a conducting liquid (e.g., water) and the bulk of the liquid; so it is measuring the electrical charges of particles suspended in a liquid. The prepared particles had positive charge ranging from 23.91 to 41.02 mV displaying the positive surface of the nanoparticles which might be resulted from the cationic amine groups on the nanochitosan surface. The value of zeta potential for all prepared nanoparticles was relatively high which indicated that the Ch-SeNPs had better colloidal stability than chitosan nanoparticles alone as well as the stability of the particles in suspension solution without agglomeration or coagulation [24].

The particles size and shapes of the synthesized chitosan nanoparticles and their nanocomposites were investigated and displayed in Fig. 3. It is clearly seen from Fig. 3a that the particles have semispherical shape with an average size about 30–40 nm with some accumulation and interconnected structure. The positively charges of amino groups of chitosan (protonated amines in aqueous acetic acid solution) interacted ionically with negatively charges of sodium tripolyphosphate developing these semi-spherical nanoparticles [31]. Figure 3b–e displays TEM for the composite nanoparticles. Selenium nanoparticle were displayed as spherical dark spots in the chitosan matrix with small particle size ranged 12–20 nm for lower concentration of selenium (Fig. 3b), whereas for Ch-Se20, the size of selenium nanoparticles was ranged of 50–75 nm (Fig. 3c). The morphology of SeNPs was spherical- like with average size of approximately 20.98 nm for Ch-Se10 and 70.74 nm for Ch-Se20. The distribution of selenium nanoparticles (dark spots) was monodispersed and showed a homogeneous structure for the lower and higher concentrations of selenium. At high concentration of selenium nanoparticles the particles might be aggregated forming relatively higher particle size.

Ch-Se-Flu was significantly affected by 5Flu concentration as shown in Fig. 3c, d. However, when the concentration of 5Flu reached 20 mg/mL; SeNPs showed a

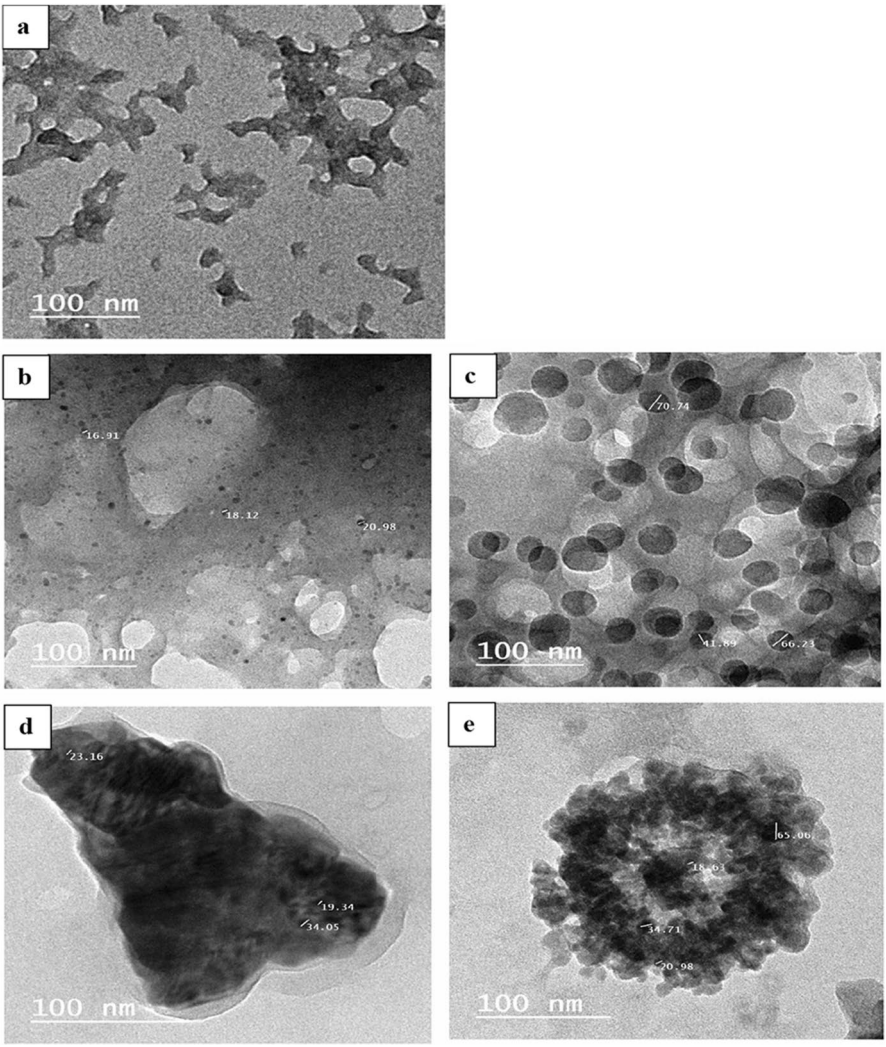

Fig. 3 TEM of **a** Ch-NP, **b** Ch-Se10, **c** Ch-Se20, **d** Ch-Se10-Flu10 and **e** Ch-Se10-Flu20

net-like structure (Fig. 3d) with aggregation of chitosan nanoparticles combined selenium and fluorouracil. The SeNPs were well cross linked and encapsulated with chitosan and 5Flu as appeared in Fig. 3c. It is worth to mention that 5-fluorouracil was well distributed and encapsulated within the Ch-Se nanoparticles with appearance of few aggregates at the outer shell of the samples. These results indicated that 5-Fu could effectively regulate the size of ChSeNPs when used in a specific range of concentrations [32]. In this context, Ch-Se10-Flu10 and Ch-Se10-Flu20 were considered promising system that can be used in drug deliver application.

The crystallinity of the prepared nanoparticles was investigated using XRD analysis as shown in Fig. 4. The XRD pattern of all nanocomposite showed a well

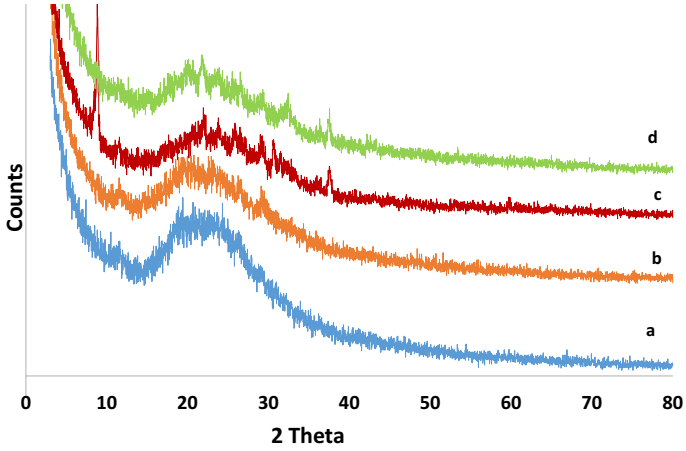

Fig. 4 XRD of **a** Ch-Se10, **b** Ch-Se20, **c** Ch-Se10-Flu10 and **d** Ch-Se10-Flu20

characteristic broad peak around 20° which related to the chitosan molecule [33]. Moreover, the XRD pattern of Se NPs displayed several Bragg's reflections. The clear peaks of cubic phases were recorded at $\theta = 22.4°$ (100), 32.50° (101), 45.80° confirming the crystalline nature of the prepared Se NPs [17, 34]. These results indicated that SeNP was not pure amorphous and had the crystalline trigonal phase of Se [34–36]. However, the peaks displayed at 19, 24 and 29° were attributed to 5-fluorouracil existence in the prepared nano-carrier [27]. These finding results illustrated the successful preparation of chitosan encapsulated selenium nanoparticles and 5flurouracil.

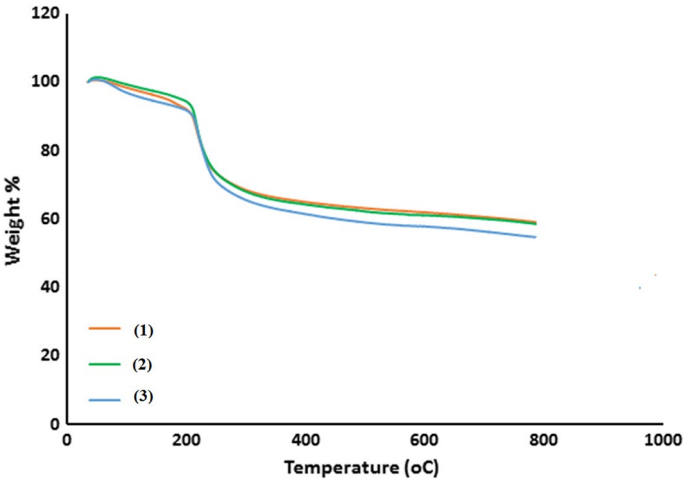

Fig. 5 TGA of (1) Ch-Se10, (2) Ch-Se20, (3) Ch-Se10-Flu10

Thermal stability of chitosan selenium nanocomposites was assessed using TGA and displayed in Fig. 5. All nanoparticles showed small weight losses (about 5%) around 100 °C due to the adsorbed moisture content. The decomposition peak at 240 °C was attributed to chitosan, with weight loss reached 36% and appeared as strong single peak. All the curves showed good thermal stability till about 800 °C. The thermal stability of these nanocomposite resulted from the presence of inorganic nanoparticles (selenium nanoparticle).

Release profile of 5-flurouracil encapsulated nanocomposite

The in-vitro release profile of 5-fluorouracil drug from chitosan selenium nanocomposite (Ch-Se10-Flu20) was performed in phosphate buffer solution with different pH (4 and 7.4) mimicking the acidic and pH of blood, respectively. It is obviously displayed in Fig. 6 that a rapid initial drug released for the first 8 h for both buffer medium which may be due to the well-known burst effect, resulted from some amounts of drugs were localized on the surface of the nanocomposite that can be easily released by diffusion. The figure indicated also the higher release of 5-flurouracil drug in the acidic medium that at pH 7.4 which may be attributed to the higher swelling performance of chitosan nanoparticles in acidic medium due to the protonated effect of amine groups in acidic medium.

After the initial rapid release, a slower continued release of 5-fluorouracil was attained within the period of 8–24 h and the release reached to about 74% after 24 h for acidic PBS medium and released about 62% in pH 7.4. The nanocomposites were stable and can retain 5-fluorouracil within their structure particularly at pH7.4 and may be need more time to be fully released. These results demonstrated that this system considered a reasonable candidate for drug delivery for cancer treatment applications.

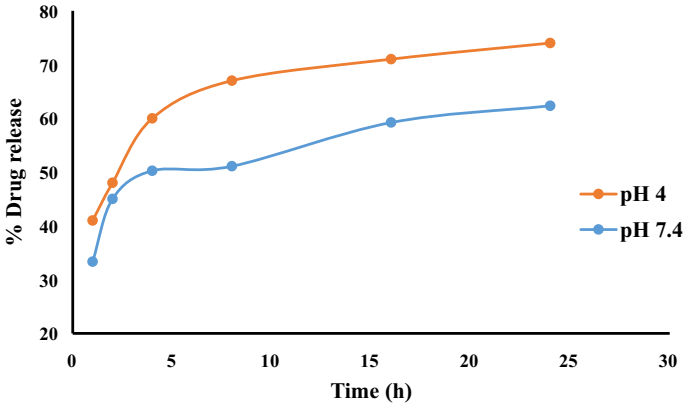

Fig. 6 In vitro release profiles of 5-Fluorouracil from nanocomposite (Ch-Se10-Flu20) in PBS solution at pH 4 and 7.4

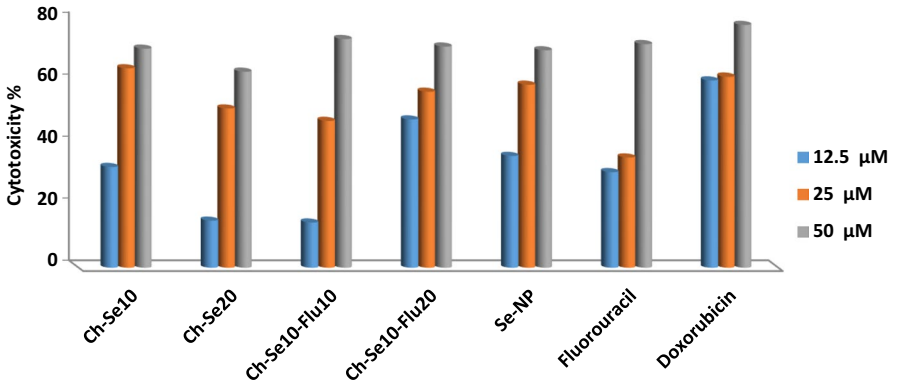

Fig. 7 Dose dependent antiproliferative data of the nano-composites and their corresponding three blanks on HCT-116 cancer cells

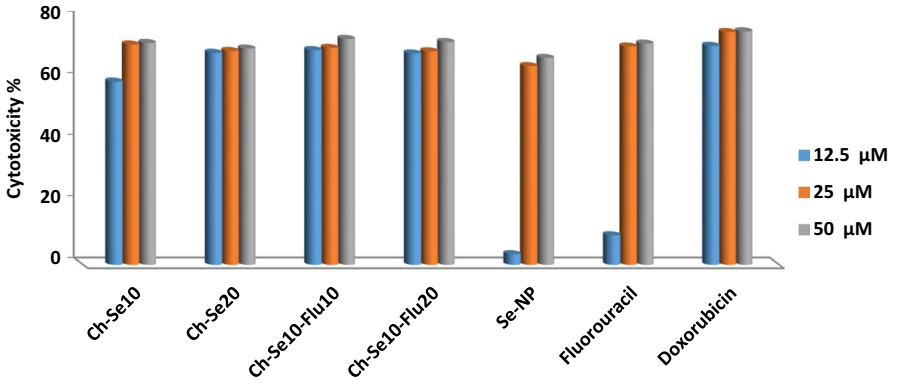

Fig. 8 Dose dependent antiproliferative data of the nano-composites and their corresponding blanks on MCF-7 cancer cells

Table 2 The antiproliferative IC_{50} of the nano-composites and their corresponding blanks on the three cancer cell lines according to the MTT assay

Compound code	IC_{50} (µM) ± SD		
	HCT-116	HepG-2	MCF-7
Ch-Se10	22.8 ± 3.1	63.1 ± 5.8	21.3 ± 2.5
Ch-Se20	36.4 ± 4.5	53.8 ± 4.9	20.4 ± 1.9
Ch-Se10-Flu10	34.2 ± 2.8	51.7 ± 3.5	19.3 ± 1.5
Ch-Se10-Flu20	19.7 ± 1.9	67.1 ± 6.1	19.9 ± 1.6
Se-NP	23.6 ± 2.1	41.5 ± 3.6	35.8 ± 3.1
Fluorouracil	33.1 ± 2.9	58.8 ± 5.1	31.9 ± 2.8
Doxorubicin	21.8 ± 2.9	63.2 ± 5.8	16.7 ± 1.5

Anticancer activity of the prepared nanocomposite

Four nano-composites in addition to 5-fluorouracil and selenium nanoparticles as blank samples were examined in vitro for their activity on HCT-116, HepG-2, MCF-7 human cancer cells and one human healthy cell line (BJ-1) using the MTT assay. The percentages of intact cells were calculated and compared to those of the control. Activities of these nano-composites against the three carcinoma cell lines were compared to the activity of doxorubicin. All nano-composites suppressed the three cancer cells in a dose-dependent manner as shown in (Figs. 7, 8). In case of HCT-116 human colorectal carcinoma cells: both Fig. 7 and Table 2 showed that three nano-composites (Ch-Se10-Flu20, Ch-Se10 and Se-NP, respectively) had comparable potent cytotoxic activities; the rest of the nanocomposites significantly exhibited moderate cytotoxic activity against HCT-116 relative to that of doxorubicin. The highest activity of nanocomposite containing relatively high concentration of 5-fluorouracil (Ch-Se10-Flu20) indicating the high effect of the well-known drug in suppressing the growth of the cancer cells [37]. 5-fluorouracil interferes with nucleic acid synthesis, inhibits DNA synthesis, and eventually stops cell growth. The high activity of composite containing Se-NP with low concentration (Ch-Se10) may be due to the smaller size of Se NP as shown in Fig. 3b compared with that containing high Se NP (Fig. 3c). Selenium nanoparticle with small size can easily penetrate from the nano-capsule into the cell line suppressing their growth [38]. In case of MCF-7 human breast cancer cells: the four nano-composites (Ch-Se10-Flu10, Ch-Se10-Flu20, Ch-Se20 and Ch-Se10%, respectively) had comparable potent cytotoxic activities; the two corresponding blanks (Fluorouracil and SeNPs, respectively) displayed moderate cytotoxic activity against MCF-7 relative to the reference drug (Fig. 8 and Table 2). The high activity of nanocomposite containing both Se-NP and 5-flurouracil attributed to the combined effect of anticancer property of both the drug and Se nanoparticles [39]. In case of HepG2 human liver cancer cells: three nano-composites and their corresponding blanks (SeNP, Ch-Se10-Flu10,

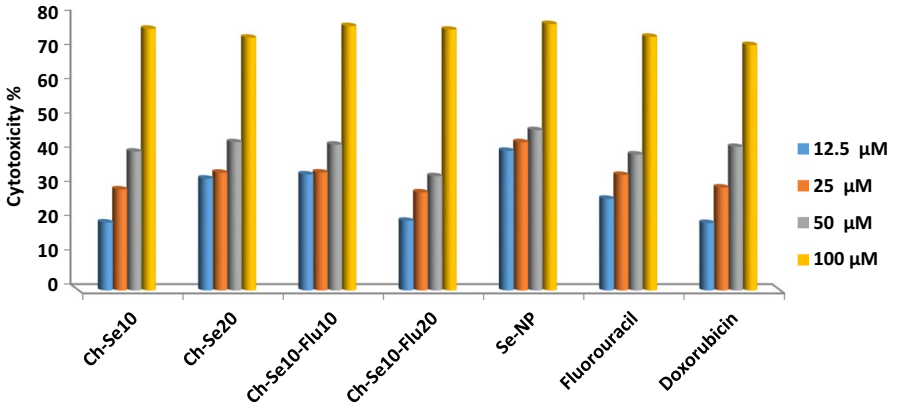

Fig. 9 Dose dependent antiproliferative data of the nano-composites and their corresponding blanks on HepG2 cancer cells

Ch-Se20, blank Flu, and Ch-Se10, respectively) showed cytotoxic activity at higher concentration of nanocomposite (100 µM) compared with their effect on the other cancer cell line at (50 µM). (Ch-Se10-Flu20) represented slight less cytotoxic activity against HepG2 relative to that of doxorubicin (Fig. 9 and Table 2). The synthesized nanocomposites have high potent effect on human breast cancer cells MCF-7 followed human colorectal carcinoma cells HCT-116 then human liver cancer cells HepG2. All compounds were tested against non-tumor fibroblast-derived cell line (BJ) and demonstrated very low cytotoxicity. It is worth to mention that the above data demonstrated that SeNPs synthesized without a stabilizer was unstable and easily agglomerate, which confirmed the important role of Ch for further 5-Flu encapsulation.

Conclusion

Novel nanocomposite system compromising from chitosan nanoparticles encapsulated selenium nanoparticles and 5-fluorouracil was successfully prepared. Characterization of the prepared nanoparticles with instrumental techniques confirmed the formation of nanoparticles with particle size ranged 207 nm for blank nano-chitosan to 250 nm for nano-chitosan containing selenium and 5-fluorouracil with positively charged surface. Distribution of the SeNPs within chitosan particle was confirmed by TEM. Application of the synthesized nanocomposite in cancer treatment was investigated against several cancer cell lines. The encapsulated nanocomposites showed potent anticancer activity towards HCT-116 human colorectal carcinoma cells, HepG2 human liver cancer cells and less activity against human breast adenocarcinoma MCF-7. All prepared composites nanoparticles were evaluated against non-tumor fibroblast-derived cell line (BJ) and displayed very low cytotoxicity. The prepared Ch-Se-NPs nanocomposite offered low cost and high efficient system that could be recommended as promising vehicle in cancer therapy.

Author contributions AEA; Conception, Material preparation, Data collection, Analysis, and writing the first draft of manuscript, EHA; Conception, Material preparation, Data collection and writing the first draft of manuscript, HMA; Cytotoxicity investigation, Data collection and revise the final manuscript, MMHA; Conception and revise the final draft of manuscript.

Funding Open access funding provided by The Science, Technology & Innovation Funding Authority (STDF) in cooperation with The Egyptian Knowledge Bank (EKB).

Declarations

Conflict of interest The authors confirm that there are no conflict of interest.

References

1. Chen W, Yue L, Jiang Q et al (2018) Synthesis of varisized chitosan-selenium nanocomposites through heating treatment and evaluation of their antioxidant properties. Int J Biol Macromol 114:751–758. https://doi.org/10.1016/j.ijbiomac.2018.03.108
2. Kołodyńska D, Hałas P, Franus M, Hubicki Z (2017) Zeolite properties improvement by chitosan modification—sorption studies. J Ind Eng Chem 52:187–196. https://doi.org/10.1016/j.jiec.2017.03.043
3. https://www.researchgate.net/publication/317152608_Chitosan_Nanoparticles-Trypsin_Interactions_Bio-physicochemical_and_Molecular_Dynamics_Simulation_Studies
4. Grenha A (2012) Chitosan nanoparticles: a survey of preparation methods. J Drug Target 20:291–300. https://doi.org/10.3109/1061186X.2011.654121
5. Nagpal K, Singh SK, Mishra DN (2010) Chitosan nanoparticles: a promising system in novel drug delivery. Chem Pharm Bull 58:1423–1430
6. Mitra S, Gaur U, Ghosh PC, Maitra AN (2001) Tumour targeted delivery of encapsulated dextran-doxorubicin conjugate using chitosan nanoparticles as carrier. J Control Release 74:317–323
7. Cao H, Xiao J, Liu H (2019) Enhanced oxidase-like activity of selenium nanoparticles stabilized by chitosan and application in a facile colorimetric assay for mercury (II). Biochem Eng J 152:107384
8. Chen W, Li Y, Yang S et al (2015) Synthesis and antioxidant properties of chitosan and carboxymethyl chitosan-stabilized selenium nanoparticles. Carbohydr Polym 132:574–581
9. Song X, Chen Y, Zhao G et al (2020) Effect of molecular weight of chitosan and its oligosaccharides on antitumor activities of chitosan-selenium nanoparticles. Carbohydr Polym 231:115689. https://doi.org/10.1016/j.carbpol.2019.115689
10. Kalishwaralal K, Jeyabharathi S, Sundar K et al (2018) A novel biocompatible chitosan–Selenium nanoparticles (SeNPs) film with electrical conductivity for cardiac tissue engineering application. Mater Sci Eng C 92:151–160
11. Bastianini S, Silvani A (2014) Keshan disease, selenium deficiency, and the selenoproteome. New Engl J Med 370:1756–1760. https://doi.org/10.1177/2514183x18789327
12. Kalishwaralal K, Jeyabharathi S, Sundar K, Muthukumaran A (2016) A novel one-pot green synthesis of selenium nanoparticles and evaluation of its toxicity in zebrafish embryos Artif. Cells Nanomed Biotechnol 44:471–477
13. Guo L, Huang K, Liu H (2016) Biocompatibility selenium nanoparticles with an intrinsic oxidase-like activity. J Nanoparticle Res 18:1–10. https://doi.org/10.1007/s11051-016-3357-6
14. https://www.researchgate.net/publication/269719051_Construction_of_selenium_nanoparticlesb-glucan_composites_for_enhancement_of_the_antitumor_activity
15. Feng Y, Su J, Zhao Z et al (2014) Differential effects of amino acid surface decoration on the anticancer efficacy of selenium nanoparticles. Dalt Trans 43:1854–1861. https://doi.org/10.1039/c3dt52468j
16. Panahi-Kalamuei M, Salavati-Niasari M, Hosseinpour-Mashkani SM (2014) Facile microwave synthesis, characterization, and solar cell application of selenium nanoparticles. J Alloys Compd 617:627–632
17. Bai K, Hong B, He J et al (2017) Preparation and antioxidant properties of selenium nanoparticles-loaded chitosan microspheres. Int J Nanomedicine 12:4527–4539. https://doi.org/10.2147/IJN.S129958
18. Ren Y, Niu M, Gu W, Fang Y (2012) Facile synthesis of trigonal selenium nanotubes in ethanol at low temperature. Mater Lett 82:148–151. https://doi.org/10.1016/j.matlet.2012.05.063
19. https://www.researchgate.net/publication/305032398_Selenium_Nanomaterials_An_Overview_of_Recent_Developments_in_Synthesis_Properties_and_Potential_Applications

20. Zhai X, Zhang C, Zhao G et al (2017) Antioxidant capacities of the selenium nanoparticles stabilized by chitosan. J Nanobiotechnology 15:1–12. https://doi.org/10.1186/s12951-016-0243-4
21. Zeng D, Zhao J, Luk K et al (2019) Potentiation of in vivo anticancer efficacy of selenium nanoparticles by mushroom polysaccharides surface decoration. J Agric Food Chem 67:2865–2876. https://doi.org/10.1021/acs.jafc.9b00193
22. Cheng L, Wang Y, He X, Wei X (2018) Preparation, structural characterization and bioactivities of Se-containing polysaccharide : a review. BIOMAC 120:82–92. https://doi.org/10.1016/j.ijbiomac.2018.07.106
23. Elgadir MA, Uddin S, Ferdosh S et al (2015) Impact of chitosan composites and chitosan nanoparticle composites on various drug delivery systems : a review. J food drug Anal 23:619–629. https://doi.org/10.1016/j.jfda.2014.10.008
24. https://www.researchgate.net/publication/269719051_Construction_of_selenium_nanoparticlesb-glucan_composites_for_enhancement_of_the_antitumor_activity
25. Pant A, Negi JS (2018) Novel controlled ionic gelation strategy for chitosan nanoparticles preparation using TPP-β-CD inclusion complex. Eur J Pharm Sci 112:180–185. https://doi.org/10.1016/j.ejps.2017.11.020
26. Ramadan M, El-Saber M, Abdelhamid A, El-Sayed A (2021) Effect of nano-chitosan encapsulated spermine on growth, productivity and bioactive compounds of chili pepper (*Capsicum annuum* L.) under salinity stress. Egypt J Chem 65:1–12. https://doi.org/10.21608/ejchem.2021.105793.4870
27. Ahmed EH, Abdelhamid AE, Vylegzhanina ME et al (2020) Morphological and spectroscopical characterization of hyperbranched polyamidoamine–zwitterionic chitosan-encapsulated 5-FU anticancer drug. Polym Bull. https://doi.org/10.1007/s00289-020-03495-8
28. Abuelizz HA, Marzouk M, Bakheit AH et al (2021) Antiproliferative and antiangiogenic properties of new VEGFR-2-targeting 2-thioxobenzo[g]quinazoline derivatives (In Vitro). Molecules. https://doi.org/10.3390/molecules25245944
29. Abd-El-Maksoud MA, El-Hussieny M, Awad HM et al (2020) Chemistry of phosphorus ylides. Part 47. Synthesis of organophosphorus and selenium pyrazolone derivatives, their antioxidant activity, and cytotoxicity against MCF7 and HepG2. Russ J Gen Chem 90:2356–2364. https://doi.org/10.1134/S1070363220120208
30. Abdel Elatif R, Shabana M, Ibrahim LF et al (2020) Chemical composition and biological activity of *salicornia fruticosa* L. Egypt J Chem 63:1713–1721. https://doi.org/10.21608/ejchem.2019.18470.2139
31. Algharib SA, Dawood A, Zhou K et al (2022) Preparation of chitosan nanoparticles by ionotropic gelation technique: Effects of formulation parameters and in vitro characterization. J Mol Struct 1252:132129. https://doi.org/10.1016/j.molstruc.2021.132129
32. Li H, Liu D, Li S, Xue C (2019) Synthesis and cytotoxicity of selenium nanoparticles stabilized by α -D-glucan from *Castanea mollissima* Blume. Int J Biol Macromol 129:818–826. https://doi.org/10.1016/j.ijbiomac.2019.02.085
33. Zidan TA, Abdelhamid AE, Zaki EG (2020) N-Aminorhodanine modified chitosan hydrogel for antibacterial and copper ions removal from aqueous solutions. Int J Biol Macromol 158:32–42. https://doi.org/10.1016/j.ijbiomac.2020.04.180
34. El-Batal AI, Mosallam FM, Ghorab MM et al (2020) Factorial design-optimized and gamma irradiation-assisted fabrication of selenium nanoparticles by chitosan and *Pleurotus ostreatus* fermented fenugreek for a vigorous in vitro effect against carcinoma cells. Int J Biol Macromol 156:1584–1599. https://doi.org/10.1016/j.ijbiomac.2019.11.210
35. Li L, Wang W, Chen K (2014) Synthesis of black elemental selenium peroxidase mimic and its application in green synthesis of water-soluble polypyrrole as a photothermal agent. J Phys Chem C 118(45):26351–26358
36. Kumar A, Sevonkaev I, Goia DV (2014) Synthesis of selenium particles with various morphologies. J Colloid Interface Sci 416:119–123. https://doi.org/10.1016/j.jcis.2013.10.046
37. Ortiz R, Prados J, Melguizo C et al (2012) 5-fluorouracil-loaded poly(ε-caprolactone) nanoparticles combined with phage E gene therapy as a new strategy against colon cancer. Int J Nanomedicine 7:95–107. https://doi.org/10.2147/ijn.s26401
38. Ramamurthy CH, Sampath KS, Arunkumar P et al (2013) Green synthesis and characterization of selenium nanoparticles and its augmented cytotoxicity with doxorubicin on cancer cells. Bioprocess Biosyst Eng 36:1131–1139. https://doi.org/10.1007/s00449-012-0867-1

39. Spyridopoulou K, Aindelis G, Pappa A, Chlichlia K (2021) Anticancer activity of biogenic selenium nanoparticles: apoptotic and immunogenic cell death markers in colon cancer cells. Cancers (Basel) 13:5335. https://doi.org/doi.org/10.3390/cancers13215335